Online microscopic calibration of train motion models: towards the era of customized control solutions

Valerio De Martinis [a, 1], Francesco Corman [a],
[a] Institute for Transport Planning and Systems IVT, ETH Zurich
P.O. 8093 Zurich, Switzerland
[1] E-mail: valerio.demartinis@ivt.baug.ethz.ch,

Abstract

The on-board collection of data related to train operation enables a better calibration of the current train motion models, which are fundamental for the elaboration of optimized train control solutions. Here, the possibility to implement an online calibration of train motion models at microscopic detail, i.e. to set the model's parameters for the single train on the go, is explored. For this purpose, a comparison of different calibration models is proposed. Then, the performances of the models are evaluated according to the requirements for online elaborations. In the end, possible further requirements and limitations on the use are discussed.

Keywords

Calibration, online, train resistances, data driven

1   Introduction

In the last years, the optimization of rail operation for different purposes (e.g., increase of network use, increase of punctuality, increase of energy efficiency) has become a primary goal for railway systems to keep being competitive in the transportation market (Corman and Meng, 2015; Rao et al. 2016). Enabling technologies and advanced modelling contribute to achieving performance goals. Nevertheless, for their effective and correct use, these must be associated with a greater specification of the models behind, to obtain more accurate results and adherence to reality.

Therefore, the calibration of train motion models is a key aspect, since these last ones constitute the backbones for the elaboration of optimized solutions for train control, such as determining precisely running time supplements, determining control actions to ensure energy saving profiles and have succession of trains at minimum separation time, in order to maximize capacity usage in bottlenecks. Some positive experiences have already shown the importance of the offline calibration (Besinovic et al., 2013). However, the variety of possible rolling stock characteristics (e.g. freight trains) and of possible operating conditions (e.g. weather conditions) limit the expected enhancements during implementation.

The sensors invasion and the consequent availability of huge dataset of on-board monitoring systems (e.g. on power used, energy consumed, speed, position, etc.) open to the opportunity to overcome these issues with a proper calibration of the train motion model. Some interesting insights have been already highlighted in recent papers, such as in Hansen et al (2016) and De Martinis and Corman (2018).

In this paper, we focused our attention on online microscopic calibration. When the train is running, we can directly determine the parameters values of the train motion model. This

allows to compute a specific control strategy for that train and to implement it on the go. In other words, there is the possibility to determine the motion model for a specific train in a specific moment, thus enabling customized train control strategies.

Main objective of this paper is therefore to investigate under which conditions an online calibration of train motion models is achievable, identify current gaps, and address possible further research. Within this work, we aim at feeding the discussion with the following contributions to the field:

- Specification of a microscopic calibration model for train motion models based on data collected on board.
- Evaluation of the performance of the proposed calibration model in relation to: track characteristics and motion phases, computation speed, number of observations.
- Discussion on possible requirements and limitations.

Finally, this paper is seen within the stream of research on automation of train control, main aim is to enhance the knowledge for future on-line calibration processes of DASs or ATP/ATO systems

A large data set provided by a Swiss train operator consisting of monitoring data collected in multiple months, related to the operation of different trains on different tracks, for many hundred trains, is used as reference.

2   Train resistances in train motion models and motion phases

Train resistances play a primary role in train operation. These largely affect train performances, travel times and energy consumptions. Travel times relate to possible saving by better exploitation of capacity, for a single train (running time reserves) and multiple trains (buffer time between minimum headway). Regarding energy consumptions, precise estimations of train resistances are needed for generating optimal train control strategies in real time. Nowadays, train resistances are computed through well-known polynomial formulations dependent upon speed (for more details, see Hansel and Pachl, 2014), some of which have been elaborated in the first decades of the last century, and sporadically updated by the scientific community, such as in Rochard and Schmidt (2000) or by train operators. Nevertheless, it usually happens that monitoring data describe a reality that cannot be totally explained by the current models; for example, Bomhauer-Beins et al. (2018) highlighted that the high variability of energy consumption between same passenger trains running on the same track with similar speed profiles can be explained by considering the weather conditions (e.g. wind, snow…).

On the other hand, the expertise acquired with the current formulation of train resistances is a valuable fix point of the train motion modeling and, at authors' knowledge, it is still the most used formulation. Generally, train motion models are used to describe the motion of a train in terms of acceleration, speed time and distance traveled. In particular, this work focuses on dynamic train motion models, which relate the forces applied to a train (tractive efforts, train resistances) with its motion. These are formulated through a dynamic approach based on Newton's second law of motion, and specified as follows:

$$F^{tr}(v) - F^{R}_{veh}(v) - F^{R}_{inf}(s) = f_t * m * dv/_{dt} \qquad (1)$$

where F^{tr} are the efforts generated by the traction unit, depending on the speed v, F^{R} are the resistances related respectively to vehicle (*veh*, dependent on speed) and to the line (*inf*,

dependent on position *s*), f_t is the mass factor, *m* is the mass of the train and *dv/dt* is the acceleration.

Line resistances (slopes and curves) are modelled as additional resistances that depend on train position. Their values depend on track characteristics (gradient and radius) and the train mass. Specifically:

$$F_{inf}^R(s) = F_{slope}^R(s) + F_{curve}^R(s) = m\,g\sin i(s) + mg\,700/r(s) \qquad (2)$$

In equation (2), the resistance given by slopes depends on the train mass *m,* the gravity acceleration *g* and the gradient *i.* When *i* is negative, slopes contribute positively to the train motion. The resistance given by curves depends on the train mass *m,* the gravity acceleration *g* and the curve radius *r.*

Equation (1) leads to a formulation of train motion that depends on train motion parameters. Specifically, the tractive efforts F^{tr} applied at wheels can be related to the active power measured at the traction unit:

$$P = \frac{1}{\eta}F^{tr}v \qquad (3)$$

Where the constant $\eta \in (0,1)$ represents the losses related to power transmission. Vehicle resistances can be computed, according to the consolidated practice, through a polynomial formulation:

$$F_{veh}^R = A + B*v + C*v^2 \qquad (4)$$

Where parameters *A, B* and *C* describe the resistances of the train. For more details please refer to [6].

Air resistances in tunnels are considered as an additional aerodynamic resistance. In particular, coefficient C of (4) is computed in open-air condition and it is increased, when the train is in a tunnel, of a quantity f_{Tun} that depends on tunnel dimensions (e.g. cross-sectional area), train dimensions and train shape (see [4] for more details). The coefficient C is therefore dependent on train position, and equation (4) can be rewritten as:

$$F_{veh}^R = A + B*v + \left(1 + f_{Tun}*\gamma(s)\right)C*v^2 \qquad (5)$$

Where γ is a dummy variable equal to 1 when the position (s) belongs to a tunnel, otherwise it is equal to 0.

Parameters A, B and C are evaluated according to empirical formulas that consider numerous variables, such as number of axles, number of vehicles, aerodynamic coefficient representing the shape of the vehicles and the cross-sectional area of the vehicles [7].

By defining the train motion model, it is possible to identify, within the train motion data set collected onboard, the train motion phases along the track, i.e. particular regimes which happen more often, like acceleration; cruising at more or less constant speed; coasting; and braking, discussed in what follows.

Acceleration

The acceleration phase is usually intended as a variation of the vehicle speed, i.e. the acceleration rate dv/dt is not null. The positive acceleration of a train is the result of the positive contribution given by the tractive efforts applied (F^{tr} >0). Possibly, specific track characteristics, e.g. a descent slope ($i(s)$ <0), can also contribute to it. When tractive efforts

are the only forces applied to the vehicle, acceleration is limited by the maximum performances of the train F_{max}^{tr} and the adhesion limits Ad:

$$\max {dv}/{dt} = \min({dv}/{dt}(F_{max}^{tr}), {dv}/{dt}(Ad)) \tag{6}$$

A negative acceleration, when tractive efforts are applied, means that the total contribution of the resistances in that part of the track is higher than the tractive efforts. In this condition, the train will decelerate until it will reach a new speed that allows for a new equilibrium state (i.e. resistances dependent on speed will be smaller, and resulting acceleration is null).

Cruising

The cruising phase is characterized by a constant speed.

$$F^{tr}(v) - F_{veh}^{R}(v) - F_{inf}^{R}(s) = 0 \tag{7}$$

In eq.7 the railway line slope is relevant. During descending slopes, it is possible that $F^{tr} < 0$, and this means that electric braking is applied to avoid acceleration. It is not known whether the mechanical braking is also applied or not.

Coasting

This phase is characterized by the train's inertial motion, without additional tractive effort. In this phase, tractive efforts are not applied and the resistances terms drive the train motion.

$$F_{veh}^{R}(v) - F_{inf}^{R}(s) = f_t * m * {dv}/{dt} \tag{8}$$

Braking

In the braking phase, tractive efforts are not applied and brakes are activated. In modern vehicles there are two main braking systems: the first is the electric braking, i.e. the power flow is inverted and the traction wheels work as fly-wheel, the second is the mechanical braking. . Electric braking is considered in terms of power generated by the traction unit (i.e. $F^{tr} < 0$), while data on mechanical braking efforts given by disc brakes are not collected. This lead to an incomplete knowledge of eq. (1).

3   The train motion model calibration

Typically, every model follows three main steps for its complete identification: specification, calibration and validation. The specification of a model results in its formulation, i.e. relations between the chosen variables by means of some parameters. The calibration phase sets the values of the parameters. The validation tests the goodness of the calibrated model in terms of adherence to reality.

Given a history of *k*-recorded on-board measurements ($k = 1... N$), i.e. data belonging to a given time window between a departure and a successive arrival at station (speed is 0 at beginning and end of this time window), the scope of the present section is to calibrate the resistance parameters values within such time window. We can vary the time window. Having a very small time window results in a slightly overdetermined problem, size of data and parameters are comparable. This might enable a better fit of the parameters in the time window, but a higher variability across two successive time windows (i.e. the parameters calibrated at time t and those calibrated at time t+1 might have very different values). A

long time window results in a largely overdetermined calibration problem, i.e. much more data than parameters. This results in larger sample deviation from the parameter values, but a more stable computation. A smaller time window is more reactive to changes in environment, a longer time window is less reactive to the same factors.

The calibration model is formulated as an optimization problem for parameters fitting. The setup of this specific problem requires the identification of the following parts:

- GoF (Goodness of Fit). It is the function that evaluates the adherence of the output of the specified model, given a set of coefficients, to a set of data used as reference (e.g. real world data collected).
- MoP (Measure of Performance). It is a variable that is used by the GoF operator for the evaluation of the model. For this work, F^{tr} has been considered as MoP.

The equation (1) is here treated with a difference equation approach. According to the time step Δt_k of the recorded observations (for instance, 1 sec), we formulate (1) as follows.

$$F^{tr}(v_k) - F_{veh}^R(v_k) - F_{inf}^R(s_k) = f_t * m * \frac{(v_{k+1} - v_k)}{\Delta t_k} \tag{4}$$

From the set N of recorded measurements, we can formulate the problem of calibrating the resistance parameters as follows:

$$(\hat{A}, \hat{B}, \hat{C}) = \text{argmin } GoF \left(F^{tr} \left(v(k), A, B, C, f_{Tun} F_{inf}^R(s_k) \right), \overline{F^{tr}}(k) \right) \forall k = 1 \dots N \tag{5}$$

subject to the following constraints:

$$F^{tr} \leq Ad = \mu_r * g * \frac{m}{n}; \ \mu_r = 0.161 + \frac{7.5}{(3.6 * v + 44)} \tag{6}$$

$$F^{tr}(v(k)) \leq F_{max}^{tr}(v(k)) \tag{7}$$

Equation (6) is related to adherence conditions, where m is the mass of the train, n is the number of motorized axes of the vehicle, g is gravity acceleration and μ_r is the adherence coefficient computed with the Curtius & Kniffler formula. Equation (7) ensures that the estimated tractive effort needed to win the resistances does not exceed the one produced by the traction unit in maximum power conditions. Here, the values of tractive efforts from the train motion model are a function of the speeds series (v_k for F_{veh}^R, v_k and v_{k+1} for variation of speed), A, B, C, f_{Tun} parameters and line resistances. Here train position is defined as the space traveled from last departure. The mass and the mass factor are considered as constant values.

4 Data set description

The data used in the current work are part of a large set of data collected by a Swiss train operator through onboard monitoring systems. Data available for each train course are:

- Onboard monitoring system. The single record of the onboard dataset is composed by time, speed, latitude and longitude position of the train (via GPS), and measurements at pantograph of power consumed and power generated. Such data is available with sampling frequency of one second.
- Track data. The single record of the track data consider each variation of value

in one or more of the following fields: radius, gradient, speed limitations (per each train category). For each variation, the position along the track is reported.

5 Experimental plan

5.1 Data and setup

Preliminary set up

For the present work, 50 runs between two consecutive stops at stations of passenger trains operating on a Swiss line have been selected. The travel time from timetable is 17 minutes, while average travel time from the monitoring system is 1024 seconds. The track is approximately 37 km long and digitally provided in LV95 Swiss coordinate system.
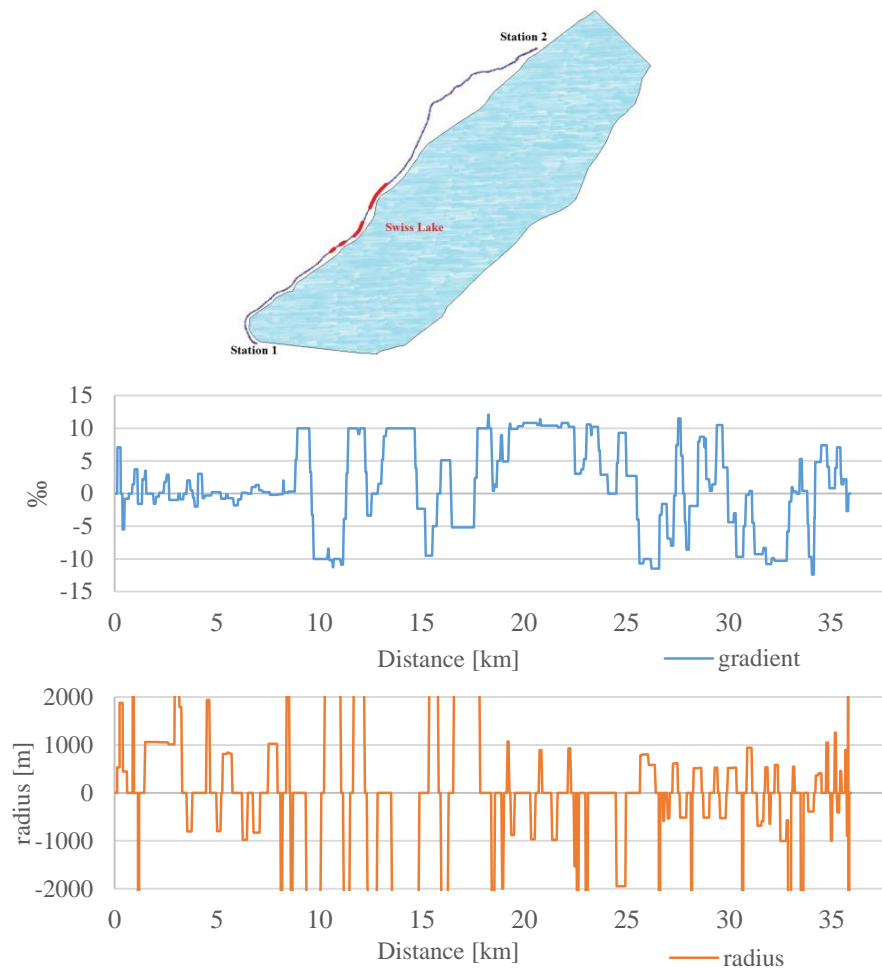
Figure 1. Top: sketch of the case study area. Middle: gradient trend along the track.
Bottom: radii trend along the track (infinite radii reported as 0 for visual representation)

Along the track there are four tunnels, respectively 0.35, 0.27, 1.25, and 2.23 km long. In Figure 1, the line development is represented (omitting names of relevant features for confidentiality). The 4 tunnels are highlighted with red thick lines. The maximum allowed velocity on the line is 160 km/h ($\cong$44.4 m/s).

The mass *m* of the train and the constant η, representing the transmission losses of power from the pantograph to the traction unit, have been given by the train operator. Data from tunnel resistances have been taken from previous empirical studies on Swiss tunnels [4; 8]. For the introduced discrete-time model, we chose the same sampling time of the recorded data $\Delta t = 1\ s$. The measured positions are taken from a reference starting point (0 m).

GoF functions

In this study, two GoF functions are evaluated according with the common knowledge in transport systems. At authors' knowledge, the calibration experiences in this railways are very few, therefore most common GoF used in other fields of transport systems, such as in traffic engineering problem (Ciuffo et al., 2012), are used:

- Sum of Absolute Error (SAE). It is the most widely used GoF for calibration in different fields. Its main characteristics is that it penalizes large errors.
- RMSE (Root Mean Square Error). It may return instabilities if there are low values along the set of data used for calibration. It is sensitive to outliers.

The tests have been made considering different time windows for calibration, namely 10, 30, 60 seconds (time-step of recorded data is 1 second), to understand calibration behavior in terms of speed and stability.

Train motion phase identification

The calibration models have been evaluated according to the different motion regimes, as described in section 2. While coasting and braking have very well defined characteristics in terms of power used (i.e. equal to zero in the first case and negative in the second case), acceleration and cruising phase can be confused; main reason is that even within the cruising phase there are some small speed deviations and related acceleration measures. This can be given by sensor noise or characteristics variability of the track which has not been reported in the input dataset.
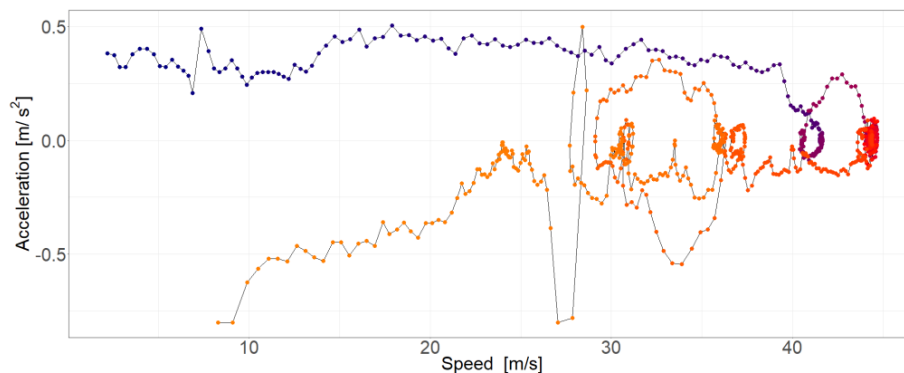
Figure 2 Acceleration vs Speed measurements

Figure 2 reports a speed/acceleration diagram of a typical train trajectory. The color indicates the evolution over space and time from the beginning (blue) to the end (orange). As shown, there are agglomerations of accelerations measurements close to zero value. These correspond to those speeds where cruising occurs; for the trajectory reported, different cruising have been performed at different speeds, like 30, 36, 42 and 44 m/s. The acceleration /braking phases, and the transition to cruising, are well distinguishable

In Figure 3, we plot a histogram of the acceleration recorded for the entire train set of train trajectories. From the acceleration values distribution (Figure 3), two bounds [-0.04, +0.04] have been set up to make the distinction between these two phases. The positive one will separate acceleration to cruising, the negative one will include some small negative accelerations that are not intended as part of the coasting phase.
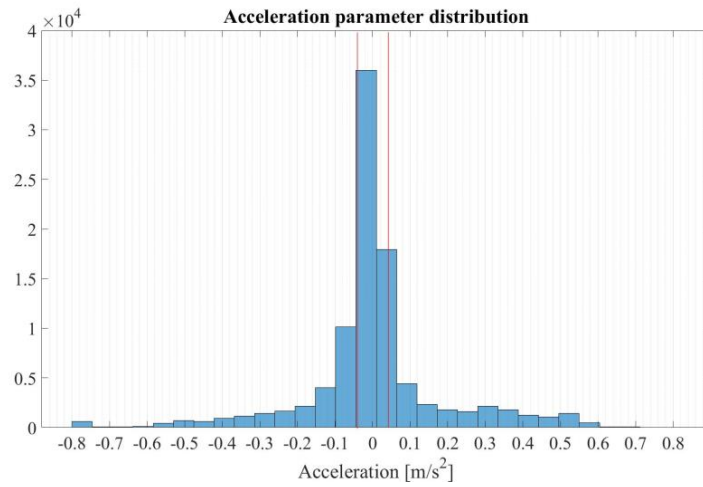
Figure 3. Acceleration measurements distribution

5.2 GoF evaluation

A first evaluation refers to the GoF function that better performs the calibration problem as specified in (5). The calibration problem has been implemented in MatLab, using the Optimization toolbox. The 2 different GoF functions have been tested with a Multi Start Gradient-based solver and 40 random starting points, to avoid being stuck in local minima. The test has been conducted considering the smallest time window of data used for calibration, i.e. 10 seconds, and a single trajectory for reference.

Results are shown in Figure 4. Here the error E_k at each step in terms of kN is reported for both the SAE and the RMSE. Specifically, the error has been evaluated through:

$$E_k = F^{tr}(v_k) - F_{veh}^R\left(\overline{A_k^{10}}, \overline{B_k^{10}}, \overline{C_k^{10}}, v_k\right) - F_{inf}^R(s_k) - f_t * m * \left.(v_{k+1} - v_k)\right/\Delta t_k$$
$$\forall k = 1 \dots N \tag{8}$$

Where $\overline{A_k^{10}}, \overline{B_k^{10}}, \overline{C_k^{10}}$ are the parameters A, B and C evaluated at time k and calibrated considering the previous 10 measurements. The error has been compared with the A, B, C values computed via Sauthoff formulation (see [6] Ch. 4 for more reference). In this latter case, it results:

$$A=2048 \ [1000*{kg*m}/{s^2}]; \ B=98,4 \ [1000*{kg}/{s}]; \ C=6,89 \ [1000*{kg}/{m}]. \quad (9)$$

From the Figure 4, the error committed with the calibrated parameters, for both the two GoF functions, is negligible when compared to the error using the classical formulation (which has errors one order of magnitude larger). In this latter case, either the formula underestimates the vehicle resistances (due to different shape of train, weight, etc.) and/or some non-modelled phenomena are affecting the train motion. An online calibration as proposed in this paper would overcome both of these issues.
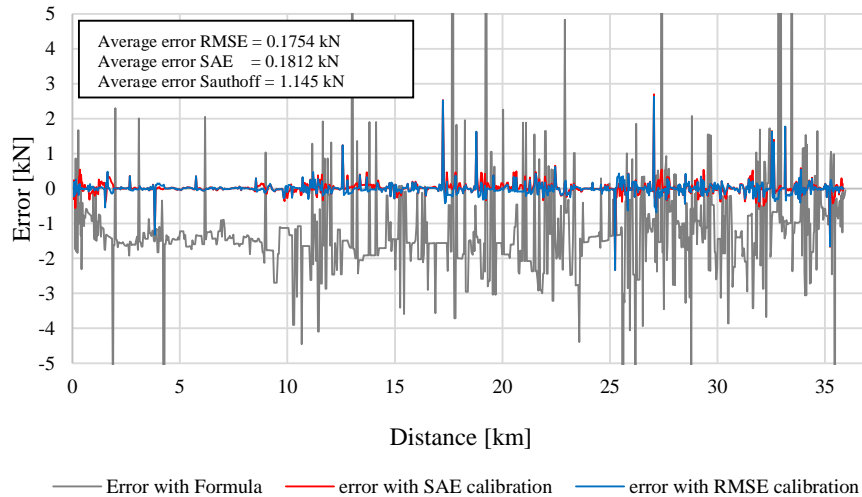
Figure 4. Error for different parameters set for a typical trajectory.

Since the results of the two GoF appear to have no substantial differences, the following elaboration will be conducted with the SAE formula. This mainly because the single iteration of the optimization process is computed faster (6.83 seconds vs 14.55 seconds).

5.3 Calibration results Inter-train characteristics

Given the calibration problem setup, calibrations on 50 different train runs have been performed. Results are shown grouped by the train motion phases as proposed before. For those phases where tractive energy is positive (energy consuming phases) results are reported, in terms of average values per train, in Figure 5 (left: acceleration; right: cruising). Results are reported as histograms of the values of the Parameters A, B and C, respectively in top, middle and bottom row of Figure 5. A kernel estimate of the distribution of values is also provided (red curve).

It is possible to note that there is a quite wide range of values between different trains both during acceleration and during cruising phase. In all cases except for B parameters in cruising phase, there is a well-defined peak value, that reflects a common characteristics among all trains at all samples. This could be for instance the similarity in train characteristics on the track, and/or the same external conditions (e.g. weather, humidity). B parameters in cruising phase have more than one peak, which may be given by a larger

influence of parameter C at higher speeds. Parameter C is well-defined in cruising phase (i.e. a clear peak in the histogram is present). This is because aerodynamics counts more at higher speeds, which are usually those used for cruising regimes.
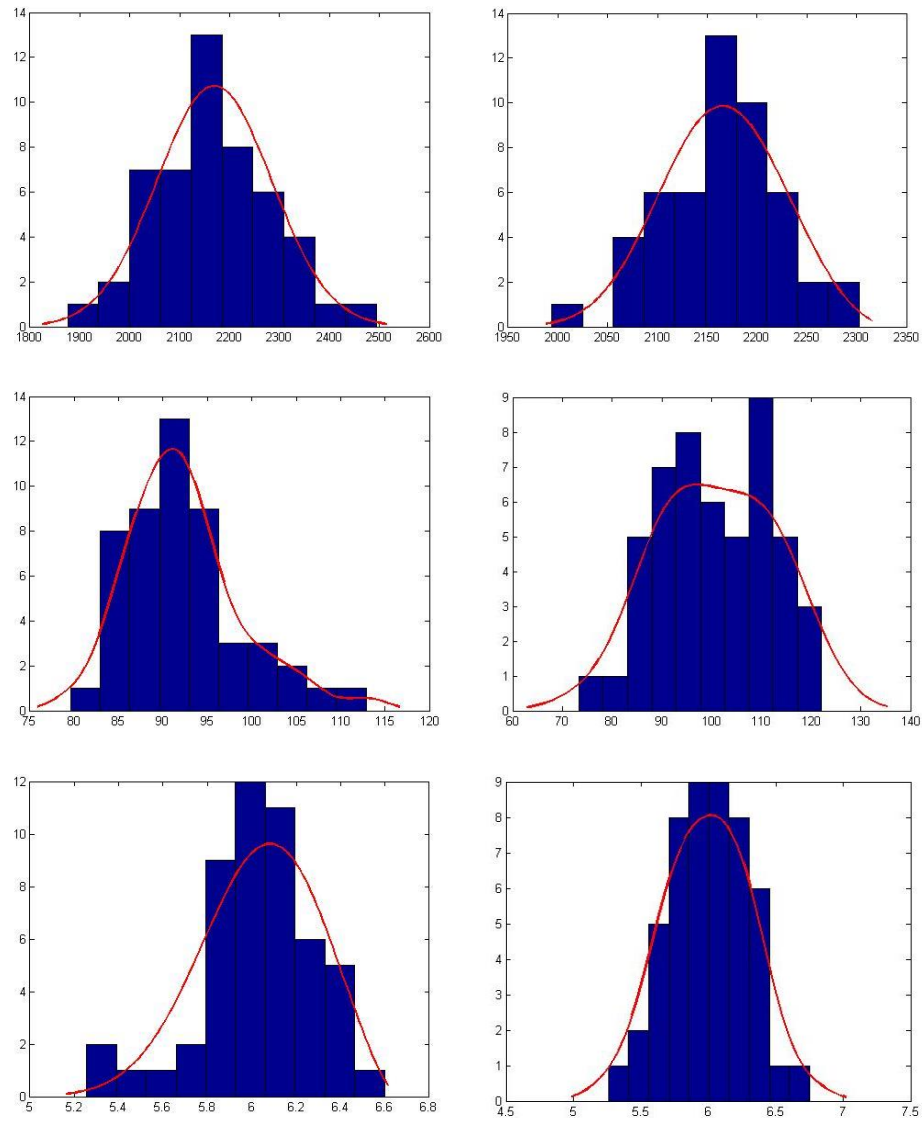
Figure 5. Parameters values distribution for the acceleration (left column) and the cruising phase (right column). Top row: A value distribution; middle row: B value distribution; Bottom row: C value distribution.
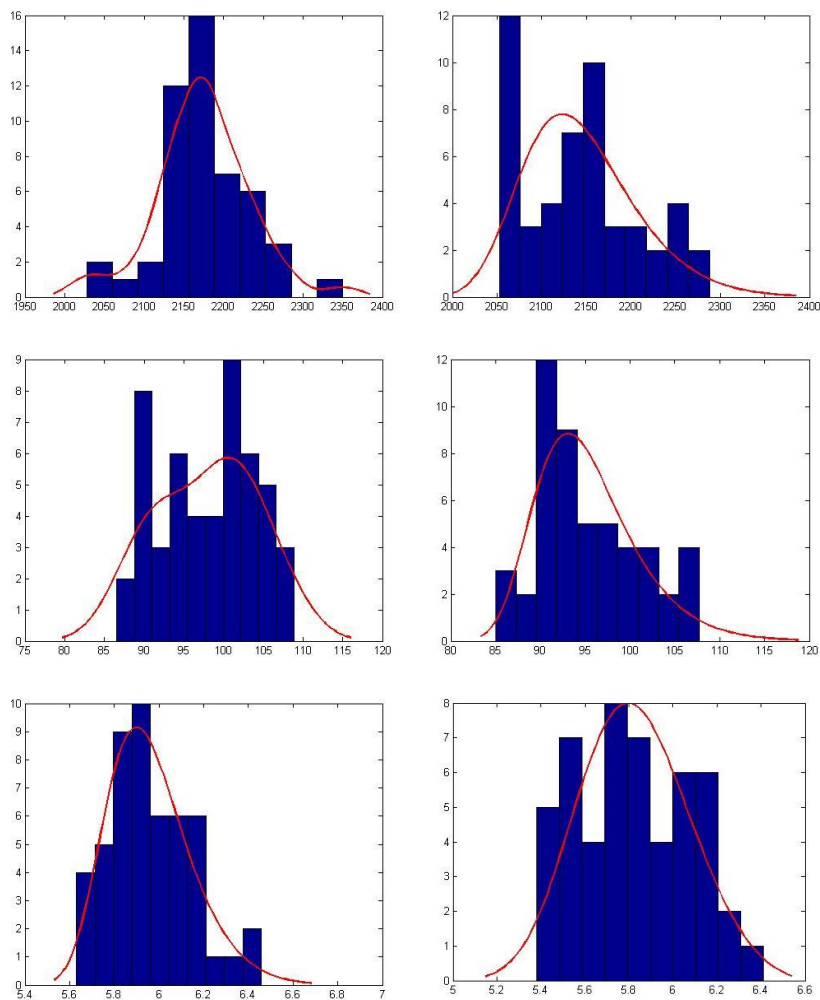
Figure 6. Parameters values distribution for the coasting (left column) and the braking phase (right column). Top row: A value distribution; middle row: B value distribution; Bottom row: C value distribution

Figure 6 shows the calibration results for those motion phases where tractive efforts were not activated, i.e. coasting (left column) and braking phase (right column). The figure shows the histogram of the computed values of A B and C (top, middle, bottom row).

Results show more than one peak of values, especially in the braking phase. This is most probably due to the missing tractive efforts information (i.e. there was no measured tractive effort) that could be considered in the optimization process. In particular B parameters of both coasting and braking phases are very sparse. Probably, the variation in one parameter reflects in the variation in the other parameters, especially B-C. In fact, issues in calibration of Parameter C can be expected, as during the braking phase resistances from the air and

resistances from the braking system work together and it is difficult to separate their working. Moreover a braking action might appear as a less aerodynamic resistance for this same reason. . Additionally, C parameters related square of speed are affected also by the small relevance of aerodynamic resistances at low speeds. Moreover, during braking phase the mechanical braking efforts are not known thus a precise estimation of resulting tractive effort is difficult.

5.4 Calibration results Intra-train characteristics

In this analysis, calibration of all considered trains is evaluated with respect of the train motion phases. Calibrations have been performed considering different time windows, i.e. the dataset for calibration had 10, 30 or 60 seconds (and an equivalent amount of samples).

We report those in Figures 7, 8 and 9, as scatter plots of the parameter estimated, along space. For each motion phase identified, we use a different color. This allows identifying variation in the distribution of the parameters, as dependent on the motion phase, and the position along the track. For each Figure, the three plots report the time window 10, 30 60 seconds, at top, middle, bottom respectively.

We start with parameter A (Figure 7), which shows bigger variances (i.e. larger spread along the vertical axis) at lower speeds (i.e. the beginning and end of the space axis), probably because the other speed-dependent parameters do not explain resistances well at lower speeds. This is associated to acceleration (green) and braking (blue) phases. Increasing the size of data set used for calibration yields, as expected, a lower variation between trains. The cruising phase (yellow) seems to give more stable evaluation along the track. This is expected since A parameter is not speed dependent.
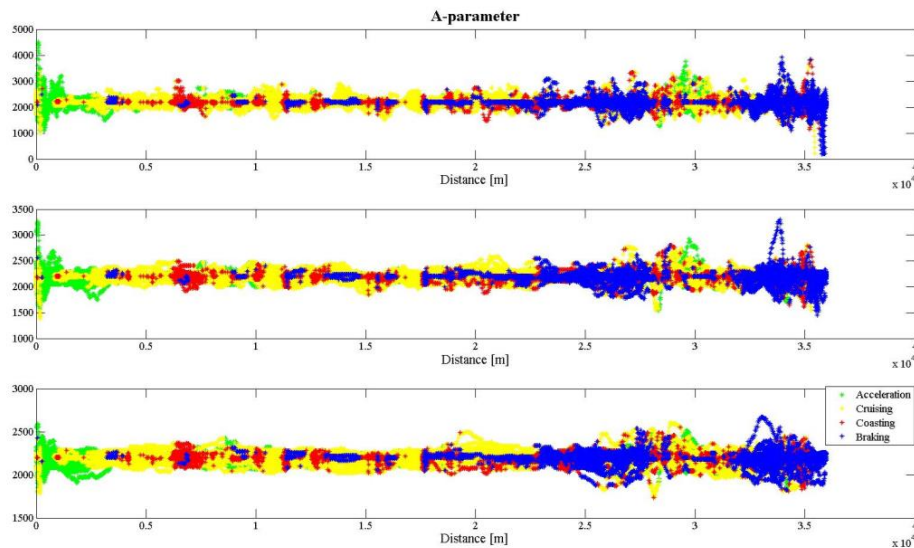
Figure 7. A-parameter values for different trains. Top: data set size is 10 seconds; middle: data set size is 30 seconds; bottom: data set size is 60 seconds
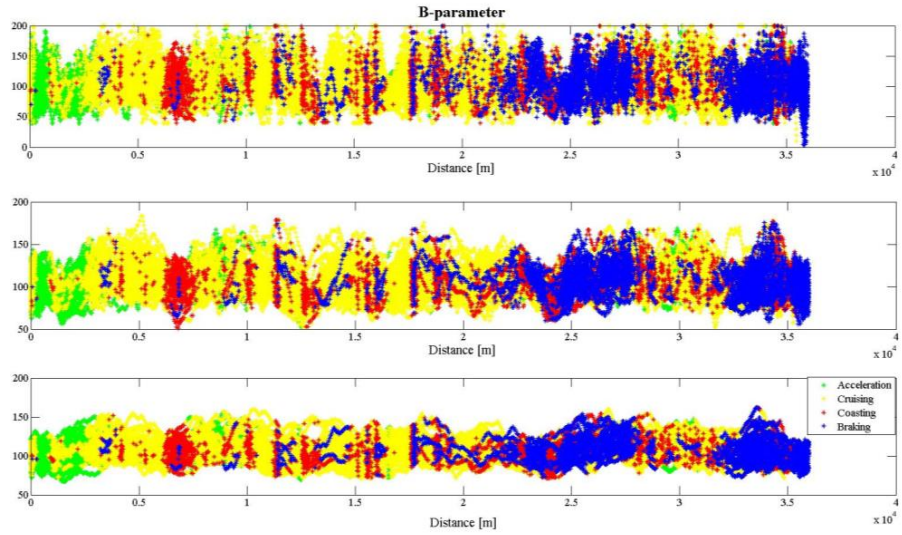
Figure 8. B-parameter values for different trains. Top: data set size is 10 seconds; middle: data set size is 30 seconds; bottom: data set size is 60 seconds
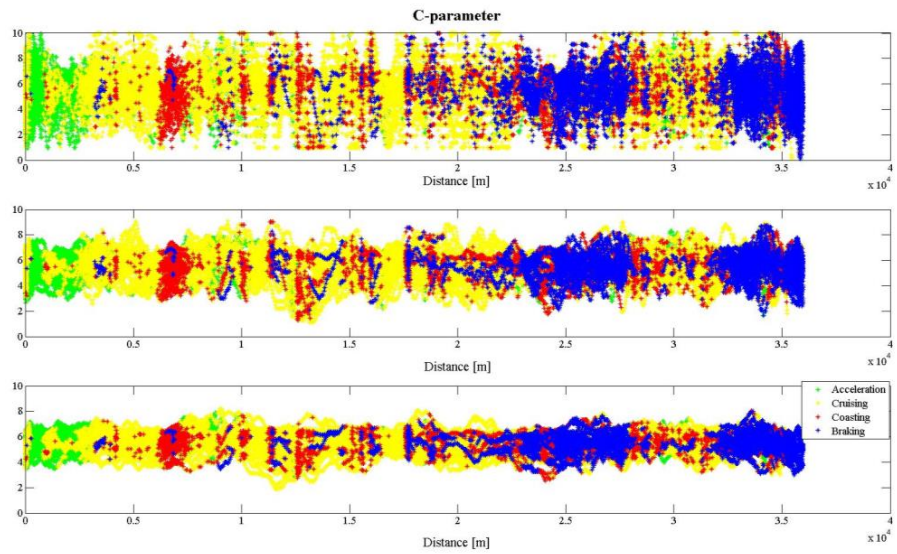
Figure 9. C-parameter values for different trains. Top: data set size is 10 seconds; middle: data set size is 30 seconds; bottom: data set size is 60 seconds

The same analysis for parameters B and C (Figure 8 and 9) shows a larger variability than parameter A, although their variability is reduced by considering a bigger set of data for calibration. Especially when analyzing the variation of parameters values with larger time windows, it is possible to see areas where the variation is lower, especially between the 15th and 20th km. On the one hand, this area corresponds to a large stretch where speed is almost constant, thus calibration is difficult. On the other hand, this suggest a possible influence of track conditions also for parameters B and C that needs further investigations. A possible idea to model variation in resistances at constant speed is to have a more rich description of the generalized resistance as dependent on the position, similar to gradients and curves. The computation times required for the different time windows used, i.e. for the optimization process for the time windows of 10, 30 and 60 seconds, are respectively 6.83, 39.2 seconds and 1 minute 12.54 seconds. In other terms, already with this preliminary implementation the optimization performed with a 10 seconds time window can be run in less than 10 seconds.

6   Recommendations, possible limitations and conclusion

This work aimed at determining the conditions under which a precise estimate of parameters of resistance of train motion can be calibrated at microscopic level (i.e. detail of one second), online (i.e. fast) and specifically per train (i.e. fitting the particular characteristics of each vehicle and train run). Within the set of experiences here presented, some interesting conclusion can be highlighted. Within the data set of trains used for this work, there is a variability between different trains and within the single runs. This can be modelled by defining appropriate set of resistances parameters A, B, C that can fit pretty well the vehicle resistances. Such a probabilistic description of train resistances would require the extension of current train running time estimation models and energy consumption estimation models to distributions rather than crisp numbers.

The calibration procedures work better in case of variation of speed, and even more, in case of positive acceleration. Assuming the current resistance formula dependent on input values of speed gradient and curvature, a variation in resistances when those three input values could not be explained. Thus, calibration of resistance parameters at cruising is particularly challenging, unless some artificial controlled variation of speed are introduced.

Keeping the trinomial formula, the physical meaning of the parameters are thus enlarged to accept non–modelled dynamics. The formula loses a bit of physical interpretation in order to describe more accurately measured resistances. A completely online approach, learning the parameters based on the data and not based on characteristics of trains such as number of axles and weight might result in better fit, but more difficult explanation to domain experts. Nonetheless, the added value of such a black-box approach, able to reduce error by an order of magnitude might well be worth it. More sophisticated calibration and /or regression techniques could be used to identify most relevant dynamics, which could be worthwhile to include in the formulation of resistance. A study of the variation of those parameters and other known unmodelled factors (for instance weather) could also be proposed.

With the proposed algorithm the online calibration for a given dataset is pretty fast. With a time window of 10 seconds of data for calibration, the values of the resistance parameters are returned in less than 7 seconds. By increasing the sample size, the stability of the parameters value over running time is increasing but the time for elaboration increases consequently.

The present work proposed the comparison of 2 main GoF, SAE and RMSE, for the

calibration process. Both alternatives perform well in the calibration procedure. The calibration with RMSE takes a longer time than with SAE, however the time required in this case (14.55 seconds) is also compatible with many online procedures (i.e. speed optimization for energy saving). Both approaches deliver error one order of magnitude lower than the formula from the books (not fitted to the specific conditions of track and train). The infrastructure itself seems to affect the calibration of the vehicle resistances, which are, in the model considered, independent from it. This suggest that possible influences are not modeled and further investigations to deepen this assumption are needed. Extension of the resistance formula might be an interesting development.

An open question is the level of accuracy for the use of online calibration in downstream systems, i.e. from traffic control to train control. This aspect cannot be treated independently, but it must be related to the technology applied and the specific type of train control strategy. Basically, continuous calibration and the variation in optimal driving strategies must consider the current driving system and the effectiveness of this variation. Considering for example energy saving train control strategies, the variation of driver's instructions, which can be enhanced by the proposed online calibration system, should be adapted to e.g. the human attitude to follow the instructions.

The main limitations are seen in the field of application, where the total time from measurement to application is relevant. We must consider: the time for data collection phase, the time for calibration, and the time for elaboration of specific solutions (e.g. for energy saving), presentation to user and/or acceptance, and the duration for implementation. This can determine lead times of multiple tens of seconds, which of course would pose requirements on the process and affect also the expected benefits. A fixed configuration of passenger trains may lead to prefer an offline procedure based on statistical evaluation of resistances parameters. Nevertheless, this means to neglect the influence of specific conditions such as weather and occupation rate of coaches. Freight trains may instead largely benefit from this online specification.

In the end the proposed model can enhance the definition of the current train motion modeling and its application to train control problems, towards more specific and accurate elaborations, such as on energy consumption estimation, braking curves, and train location, which are important key aspects for the next generation rail operation.

Acknowledgement

References

[1]. Corman, F., Meng, L., 2015. "A review of online dynamic models and algorithms for railway traffic management". *IEEE Transactions on ITS*, 16 (3), pp. 1274-1284

[2]. Rao, X., Montigel, M. and Weidmann, U., 2016. "A new rail optimisation model by integration of traffic management and train automation". *Transportation Research Part C: Emerging Technologies*, vol. 71, pp. 382-405.

[3]. Bešinović, N., Quaglietta, E., Goverde, R.M.P., 2013. "A simulation-based optimization approach for the calibration of dynamic train speed profiles". *Journal of Rail Transport Planning and Management*, vol. 3 (4), pp. 126-136.

[4]. Hansen, H.S., Nawaz, M.U. and Olsson, N., 2016. Using operational data to estimate the running resistance of trains. Estimation of the resistance in a set of Norwegian tunnels. *Journal of Rail Transport Planning and Management*, vol. 7, pp. 62-76.

[5]. De Martinis, V., Corman, F., 2018. "Data-driven perspectives for energy efficient operations in railway systems: Current practices and future opportunities". *Transportation Research Part C: Emerging Technologies*, vol. 95, pp. 679-697,

[6]. Hansen, I. A., Pachl, J., 2014. *Railway Timetabling & Operations*. Hamburg: Eurailpress.

[7]. Rochard, B. P., Schmid, F. 2000. "A review of methods to measure and calculate train resistances". *Proceedings of the Institution of Mechanical Engineers, Part F: Journal of Rail and Rapid Transit*, vol. 214 (4), pp. 185-199.

[8]. Bomhauer-Beins, A., Weidmann, U., Schranil, S., 2018. Estimation of the energy saving potential of automation in railway operations [Abschätzung des Energiesparpotentials der Automatisierung im Bahnbetrieb]. *EB - Elektrische Bahnen*, vol. 116 (4-5), pp. 150-156.

[9]. Ciuffo, B., Punzo, V., Montanino, M., 2012 The Calibration of Traffic Simulation Models : Report on the assessment of different Goodness of Fit measures and Optimization Algorithms MULTITUDE Project – COST Action TU0903. Available at: http://publications.jrc.ec.europa.eu/repository/handle/JRC68403